J|A|C|S ARTICLES

Published on Web 11/30/2009

Elucidating the Bimodal Acid−Base Behavior of the Water−Silica Interface from First Principles

Kevin Leung,*,† Ida M. B. Nielsen,‡ and Louise J. Criscenti†

Sandia National Laboratories, MS 1415 and 1322, Albuquerque, New Mexico 87185 and Sandia National Laboratories, MS 9158, Livermore, California 94551

Received July 23, 2009; E-mail: kleung@sandia.gov

Abstract: Understanding the acid−base behavior of silica surfaces is critical for many nanoscience and bionano interface applications. Silanol groups (SiOH) on silica surfaces exhibit two acidity constants—one as acidic as vinegar—but their structural basis remains controversial. The atomic details of the more acidic silanol site govern not just the overall surface charge density at near neutral solution pH but also how ions and biomolecules interact with and bind to silica immersed in water. Using ab initio molecular dynamics simulations and multiple representative crystalline silica surfaces, we determine the deprotonation free energies of silanol groups with different structural motifs. We show that previously proposed motifs related to chemical connectivity or intersilanol hydrogen bonds do not yield high acidity. Instead, a plausible candiate for $pK_a = 4.5$ silanol groups may be found in locally strained or defected regions with sparse silanol coverage. In the process, irreversible ring-opening reactions of strained silica trimer rings in contact with liquid water are observed.

I. Introduction

Deprotonation of silanol (SiOH) groups[1,2] at water−silica interfaces is one of the most common and important, yet intriguing, interfacial chemical reactions. Silica (SiO_2) is a major component of rocks and lines the channels of many nanofluidic devices.[3−5] Deprotonation governs dissolution rates,[1] affects lipid binding to silica nanostructures,[4] creates negative surface charges that can be tuned with moderate changes in solution pH to perform ion gating,[5] and may even hinder extraction of positively charged crude oil components[6] from underground deposits. In particular, the atomic level structural details of deprotonated SiOH groups govern both the overall surface charge density and the binding of ions and molecules to immersed silica surfaces. In this work, we apply ab initio molecular dynamics[7] (AIMD), which takes into account proton dynamics and hydrogen-bond network fluctuations in liquid water essential to acid−base reactions in small molecules[8−11] as well as cooperative hydroxyl hydrogen-bonding behavior specific to oxide surfaces,[12,13] to investigate the enigmatic SiOH deprotonation equilibrium constant as a function of structural motifs.

Measurements of interfacial pK_a (defined as $-\log_{10} K_a$, where K_a is the acid dissociation constant) have been revolutionized by surface-sensitive second-harmonic generation (SHG) and sum frequency vibrational spectroscopy (SFVS) techniques.[14,15] In 1992, Ong et al.[16] demonstrated that 19% of silanol groups on fused silica surfaces exhibit a pK_a of 4.5, about the same as vinegar (acetic acid), while 81% exhibit $pK_a = 8.5$. SFVS experiments on α-quartz reached similar conclusions and further suggested that the low-acidity silanol groups reside in regions with strong water−water hydrogen bonds.[17] A titration study on silica gel (amorphous silica)[18] and X-ray photoelectron spectroscopy measurements on quartz[19] also independently demonstrated the existence of SiOH groups with pK_a between 4 and 5.5. Such qualitative agreement on different forms of silica is expected because liquid water is known to react with even crystalline silica to form an amorphous layer.[2,20] These mea-

† Sandia National Laboratories, New Mexico.
‡ Sandia National Laboratories, California.

(1) Brinker, C. J.; Scherer, G. W. *Sol-Gel Science*; Academic Press: London, 1990; Chapter 10.
(2) Iler, R. K. *The Chemistry of Silica: Solubility, Polymerization, Colloid and Surface Properties, and Biochemistry*; Wiley: New York, 1979.
(3) Stein, D.; Kruithof, M.; Dekker, C. *Phys. Rev. Lett.* **2004**, *93*, 035901.
(4) Baca, H. K.; Ashley, C.; Carnes, E.; Lopez, D.; Flemming, J.; Dunphy, D.; Singh, S.; Chen, Z.; Liu, N. G.; Fan, H. Y.; Lopez, G. P.; Brozik, S. M.; Werner-Washburne, M.; Brinker, C. J. *Science* **2006**, *313*, 337.
(5) Fan, R.; Huh, S.; Yan, R.; Arnold, J.; Yang, P. D. *Nat. Mater.* **2008**, *7*, 303.
(6) Kokal, S.; Tang, T.; Schramm, L.; Sayegh, S. *Colloids Surf. A: Physicochem. Eng. Aspects* **1995**, *94*, 253.
(7) Car, R.; Parrinello, M. *Phys. Rev. Lett.* **1985**, *55*, 2471.
(8) Sprik, M. *Chem. Phys.* **2000**, *258*, 139.
(9) Ivanov, I.; Chen, B.; Raugei, S.; Klein, M. L. *J. Phys. Chem. B* **2006**, *110*, 6365.
(10) Park, J. M.; Laio, A.; Iannuzzi, M.; Parrinello, M. *J. Am. Chem. Soc.* **2006**, *128*, 11318.
(11) Geissler, P. L.; Dellago, C.; Chandler, D.; Hutter, J.; Parrinello, M. *Science* **2001**, *291*, 2121.
(12) Leung, K.; Rempe, S. B.; Lorenz, C. D. *Phys. Rev. Lett.* **2006**, *96*, 095504.
(13) Hass, K. C.; Schneider, W. F.; Curioni, A.; Andreoni, W. *Science* **1998**, *282*, 265.
(14) Eisenthal, K. B. *Chem. Rev.* **2006**, *106*, 1462.
(15) Shen, Y. R.; Ostroverkhov, V. *Chem. Rev.* **2006**, *106*, 1140.
(16) Ong, S. W.; Zhao, X. L.; Eisenthal, K. B. *Chem. Phys. Lett.* **1992**, *191*, 327.
(17) Ostroverkhov, V.; Waychunas, G. A.; Shen, Y. R. *Phys. Rev. Lett.* **2005**, *94*, 046102.
(18) Allen, L. H.; Matijevic, E.; Meites, L. *J. Inorg. Nucl. Chem.* **1971**, *33*, 1293.
(19) Duval, Y.; Mielczarski, J. A.; Pokrovsky, O. S.; Mielczarski, E.; Ehrhardt, J. J. *J. Phys. Chem. B* **2002**, *106*, 2937.
(20) Li, I.; Bandara, J.; Shultz, M. J. *Langmuir* **2004**, *20*, 10474.

10.1021/ja906190t

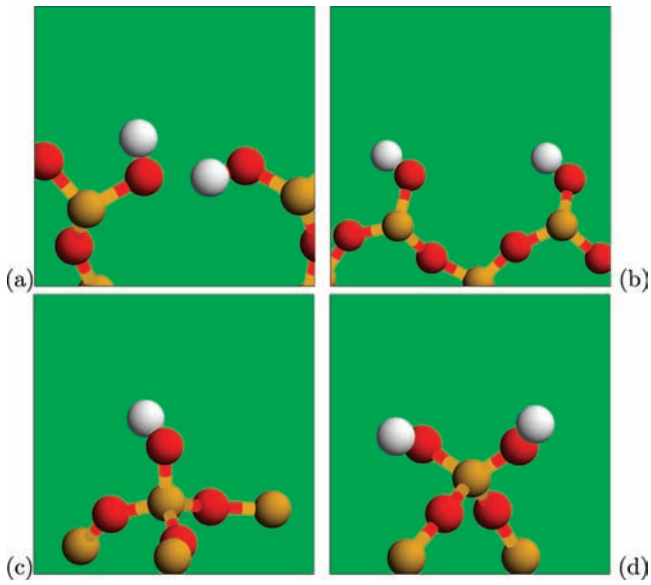

Figure 1. (a−d) Four types of SiOH groups discussed in this work: (a) hydrogen bonded, (b) isolated, (c) Q^3, and (d) Q^2. Oxygen, silicon, and hydrogen atoms are colored in yellow, red, and white, respectively.

surements suggest that the earlier, single $pK_a \sim 6.8$ reported in amorphous silica titration experiments[21] may reflect a composite of two types of SiOH.

The acidities of surface silanol groups have been assigned to different chemical connectivities or intersilanol hydrogen bonding. Following the literature, we differentiate SiOH groups according to whether they are directly hydrogen bond to other SiOH ("H-bonded", Figure 1a) or are not so hydrogen bonded ("isolated", Figure 1b), whether the 4-coordinated Si atom of the SiOH is part of 3 covalent Si−O−Si− linkages ("Q^3", Figure 1c) or only part of 2 Si−O−Si ("Q^2", Figure 1d). It has been suggested that the ratio of H-bonded to isolated SiOH is about 1:4, similar to the relative occurrence of $pK_a = 4.5$ and 8.5;[16] thus, $pK_a = 4.5$ has been ascribed to isolated silanol groups.[16,22−24] On the other hand, the Q^2:Q^3 ratio has also been described as either approximately 1:4 or 4:1, which has prompted assignment of the $pK_a = 4.5$ SiOH group to either Q^2 (refs 25 and 26) or Q^3 (refs 27−29). The conflicting estimates of the ratios of silanol groups with different structural motifs[25−29] likely reflect the difficulty brought about by the tendency of liquid water to react with crystalline silica.[20] One indisputable experimental finding is that the silanol surface density is $\sigma_{SiOH} \sim 4.6$ nm^{-2} on well-soaked amorphous samples.[2,30] On the theoretical side, static geochemical models,[31,32] which do not account for aqueous-phase hydrogen bonding and dynamical proton motion, have also been applied, but they have not yet explained the two observed acidity constants,[16−18] while quantum chemistry or DFT methods with a dielectric continuum treatment of the bulk water environment have been limited to calculating the pK_a of small silica fragments.[33−35] DFT modeling of amorphous silica slabs has also been considered,[36] but the pK_a estimates therein often do not treat water explicitly or dynamically. (See Supporting Information for discussions of the significance of hydrogen-bond network fluctuations and excess proton hopping.)

AIMD simulations have successfully reproduced the pK_a of molecules in aqueous solution[8−10] and should be particularly well suited for distinguishing *relative* SiOH pK_a that are 4 pH units apart in different environments, provided we can demonstrate that reproducible pK_a for chemically equivalent SiOH's can be predicted. Coupled with static high-level quantum chemistry corrections, they provide the most rigorous predictions for liquid-state reactions. As computing power has increased, AIMD modeling of liquid water−material interfaces has become viable,[12,13,37−41] although it remains costly because water dynamics is slower at interfaces.[42,43] Furthermore, investigation of multiple reaction sites and/or crystalline facets is often necessary when dealing with material surfaces. In this work, we study the bimodal acid−base behavior of silanol groups[16−18] by performing AIMD simulations to directly calculate the pK_a value. Given the absence of well-defined water−crystalline silica interfaces[20] and the fact that the precise atomic structure of amorphous silica surfaces is unknown, we examine six distinct, representative silanol environments. These include hydroxylated β-crystobalite (100) (Figure 2a), hydroxylated β-cristobalite (100) with one SiOH removed (Figure 2b), reconstructed β-cristobalite (100) (Figure 2c), a molecular system (Figure 2e), and two distinct SiOH on reconstructed quartz (0001) (Figure 2f). They represent the SiOH motifs proposed to be responsible for $pK_a = 4.5$ or 8.5 in the literature (Figure 1a−d).

II. Computational Methods

AIMD simulations apply the Perdew−Burke−Ernezhof (PBE) functional,[44] the Vienna Atomic Simulation Package (VASP),[45,46] a 400 eV energy cutoff, Γ-point sampling of the Brillouin zone, deuterium mass for all protons, and a 0.375 fs time step at each Born−Oppenheimer dynamics time step. The trajectories are

(21) von Schindler, P.; Kamber, H. R. *Helv. Chim. Acta* **1968**, *51*, 1781.
(22) Dong, Y.; Pappu, S. V.; Xu, Z. *Anal. Chem.* **1998**, *70*, 4730.
(23) Lorenz, C. D.; Crozier, P. S.; Anderson, J. A.; Travesset, A. *J. Phys. Chem. C* **2008**, *112*, 10222.
(24) Fan, H.-F.; Li, F. P.; Zare, R. N.; Lin, K.-C. *Anal. Chem.* **2007**, *79*, 3654.
(25) Mori, T.; Kuroda, Y.; Yoshikawa, Y.; Nagao, M.; Kittaka, S. *Langmuir* **2005**, *18*, 1595.
(26) Vance, F. W.; Lemon, B. I.; Ekhoff, J. A.; Hupp, J. T. *J. Phys. Chem. B* **1998**, *102*, 1845.
(27) O'Reilly, J. P.; Butts, C. P.; I'Anson, I. A.; Shaw, A. M. *J. Am. Chem. Soc.* **2005**, *127*, 1632.
(28) Fisk, J. D.; Batten, R.; Jones, G.; O'Reilly, J. P.; Shaw, A. M. *J. Phys. Chem. B* **2005**, *109*, 14475.
(29) Rosenholm, J. M.; Czuryskiewicz, T.; Kleitz, F.; Rosenholm, J. B.; Linden, M. *Langmuir* **2007**, *23*, 4315.
(30) Zhuravlev, L. T. *Colloids Surf. A* **2000**, *173*, 1.
(31) See, for example: Hiemstra, T.; De Wit, J. C. M.; Van Riemsdijk, W. H. *J. Colloid Interface Sci.* **1989**, *133*, 105, and references therein.
(32) Bickmore, B. R.; Tadanier, C. J.; Rosso, K. M.; Monn, W. D.; Eggett, D. L. *Geochim. Cosmochim. Acta* **2004**, *68*, 2025.
(33) Tossell, J. A.; Sahai, N. *Geochim. Cosmochim. Acta* **2000**, *64*, 4097.
(34) Rustad, J. R.; Dixon, D. A.; Kubicki, J. D.; Felmy, A. R. *J. Phys. Chem. A* **2000**, *104*, 4051.
(35) Sefcik, J.; Goddard, W. A. *Geochmim. Cosmochim. Acta* **2001**, *65*, 4435.
(36) See, for example: Tielens, F.; Gervais, C.; Lambert, J. F.; Mauri, F.; Costa, D. *Chem. Mater.* **2008**, *20*, 3336, and references therein.
(37) Nair, N. N.; Schreiner, E.; Marx, D. *J. Am. Chem. Soc.* **2008**, *130*, 14148.
(38) Cicero, G.; Grossman, J. C.; Schwegler, E.; Gygi, F.; Galli, G. *J. Am. Chem. Soc.* **2008**, *130*, 1871.
(39) Kuo, I.-F. W.; Mundy, C. J. *Science* **2004**, *303*, 658.
(40) Kudin, K. N.; Car, R. *J. Am. Chem. Soc.* **2008**, *130*, 3915.
(41) Liu, L.-M.; Krack, M.; Michaelides, A. *J. Chem. Phys.* **2009**, *130*, 234702.
(42) Takahara, S.; Sumiyama, N.; Kittaka, S.; Yamaguchi, T.; Bellissent-Funel, M. C. *J. Phys. Chem. B* **2005**, *109*, 11231.
(43) Lee, S. H.; Rossky, P. J. *J. Chem. Phys.* **1994**, *100*, 3334.
(44) Perdew, J. P.; Burke, K.; Ernzerhof, K. M. *Phys. Rev. Lett.* **1996**, *77*, 3865.
(45) Kresse, G.; Joubert, D. *Phys. Rev. B* **1999**, *59*, 1758.
(46) Kresse, G.; Furthmüller, J. *Phys. Rev. B* **1996**, *54*, 11169–11186.

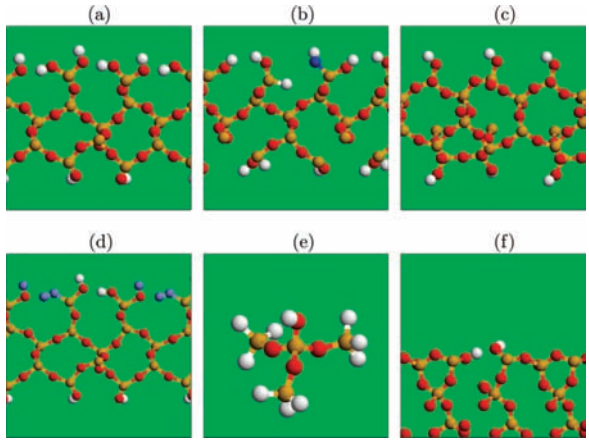

Figure 2. Heterogeneous SiOH environments examined in this work. (a) Hydroxylated β-cristobalite (100) surface. The SiOH groups have $\sigma_{SiOH} \sim 8$ nm^{-2} and are Q^2 and H bonded ($pK_a = 7.6 \pm 0.3$). (b) Hydroxylated β-cristobalite (100) surface with one SiOH group replaced with a SiH to break the chain of hydrogen bonds. The tagged (deep blue) SiOH (Q^2 and isolated) exhibits $pK_a = 8.9 \pm 0.3$. (c) Reconstructed β-cristobalite (100) surface, $\sigma_{SiOH} \sim 4$ nm^{-2}, Q^3, and isolated; $pK_a = 8.1 \pm 0.5$ (6 layers of water) and 7.0 ± 0.4 (4 layers). (d) The structure in panel c comes from removing atoms shown here in blue and attaching the resulting undercoordinated Si and O atoms. Panels a−d represent ~1.5 simulation cells in the lateral direction. (e) $(H_3SiO)_3$ SiOH, which is Q^3 and isolated, exhibits $pK_a = 7.9 \pm 0.5$. (f) Top half of a reconstructed quartz (0001) surface model containing cyclic silica trimers (Si−O)$_3$, $\sigma_{SiOH} \sim 2.3$ nm^{-2}, Q^3, and H bonded; one SiOH resides on a trimer ring ($pK_a = 5.1 \pm 0.3$); the other does not ($pK_a = 3.8 \pm 0.4$ and 4.8 ± 0.4 depending on whether a nearby trimer ring breaks; see text). Si, O, and H atoms are in yellow, red, and white, respectively. (b and e) Finite-temperature AIMD snapshots with water molecules omitted for clarity; (a, c, and f) Shown at $T = 0$ K.

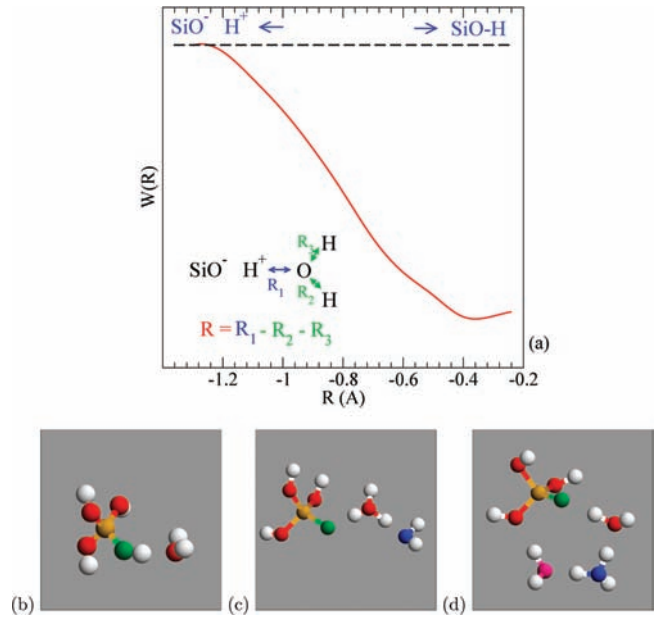

Figure 3. (a) Four-atom reaction coordinate R, illustrated for silicic acid in water but is similar for all silanol-containing species. (b−d) Snapshots from AIMD deprotonation simulations with outershell H_2O molecules removed for clarity reasons. As deprotonation proceeds, R progresses from intact SiO−H ($R \sim -0.4$ Å, panel b) to the $SiO^-H_3O^+$ contact ion pair ($R \sim -1.0$ Å, panel c) and then via a Grotthuss proton transfer to a solvent-separated SiO^-/H_3O^+ pair ($R \sim -1.32$ Å, panel d). Yellow, red, white, and green spheres represent Si, O, H, and the "O$^-$" atoms, respectively. Additionally, the water O atoms which are second and third nearest neighbors to the SiO^- oxygen are colored blue and pink, respectively. pK_a predictions for silicic acid will be reported in a future publication.

thermostat at $T = 425$ K; elevated temperature is needed to represent liquid water properties when the PBE functional is applied and quantum nuclear effects are neglected, which is the case herein (Supporting Information, section S1). Four to six umbrella sampling windows of 20 ps production trajectory length each are used per pK_a calculation on hydroxylated β-cristobalite (100) (Figure 2a and 2b) and reconstructed β-cristobalite (Figure 2c) surfaces. These periodically replicated simulation cells measure $10.17 \times 10.17 \times 26$ Å^3. Their lateral dimensions are commensurate with simulation cells often used for AIMD studies of pure water structure or ion hydration. This is one of the reasons we focus on the (100) rather than the (111) surface of β-cristobalite, which actually has a σ_{SiOH} similar to that of amorphous silica.[2] The more computationally costly reconstructed quartz (0001) system has a cell size of $10.0 \times 17.32 \times 24$ Å^3, and 12−18 ps trajectories are used per window. For each crystalline silica simulation cell, we always start from crystal slab structures optimized at zero temperature using density functional theory (DFT) and the PBE functional.[44] Next, we switch to the CHARMM SiO_2 force field[47] and the SPC/E model for water.[48] The number of water molecules occupying the simulation cell is determined using these force fields, the Grand Canonical Monte Carlo (GCMC) technique, and the Towhee code.[49] With this approach, the spaces between hydroxylated and reconstructed β-cristobalite surfaces are filled with 58 and 63 water molecules, respectively, which amount to roughly six layers of water, while the reconstructed quartz simulation cell contains about 63 (about 4 layers of) water molecules. The $(H_3SiO)_3SiOH$ pK_a calculation utilizes a $(12.42$ Å$)^3$ cell with 57 H_2O and 20 ps sampling trajectories. Finally, to check system size dependences, umbrella sampling simulations for a smaller reconstructed β-cristobalite (100) simulation cell, 20 Å in the z direction and containing 44 (4 layers of) water molecules, are also conducted for at least 10 ps per window.

The pK_a has been reported for molecules in liquid water using the AIMD technique.[8−10] It is related to the standard-state deprotonation free energy $\Delta G^{(0)}$ via $-\log_{10} \exp(-\beta \Delta G^{(0)})$, where β is $1/k_BT$ and

$$\Delta G^{(0)} = -k_B T \ln\left\{C_0 \int_0^{R_{cut}} dR A(R) \exp[-\beta \Delta W(R)]\right\} \quad (1)$$

Here C_0 denotes 1.0 M concentration, R is the reaction coordinate, $A(R)$ is a phase space factor to be discussed below, R_{cut} is the cutoff distance delimiting the reaction and product valleys in the free energy landscape, and $W(R)$ is the potential of mean force which provides the information needed to compute the free energy of deprotonation. Regardless of the reaction coordinate used,[8,9] $W(R)$ generally do not exhibit turning points in the deprotonated region and R_{cut} can be taken as the onset of the plateau where $W(R) \rightarrow 0$.

The umbrella sampling method[50] is used to compute the $W(R)$ associated with SiOH deprotonation. A four-atom reaction coordinate R (Figure 3a) is found to work best under our simulation conditions. It controls what we call the "wandering proton" problem. We label the first, second, and third neighbor H_2O molecules of the SiO^- oxygen (green sphere) shown in Figure 3b−d "water 1" (O depicted red), "2" (blue), and "3" (pink). When $R \sim -0.4$ Å (Figure 3b), the SiOH bond is intact. As R decreases to ca. -1.1 Å (Figure 3c), the SiOH proton is transferred to a "water 1" which has been hydrogen bonded to the SiOH group, yielding a $SiO^--H_3O^+$ contact ion pair. As R further decreases (Figure 3d), a proton originally residing on "water 1" is now transferred to a

(47) Lopes, P. E. M.; Murashov, V.; Tazi, M.; Demchuk, E.; MacKerell, A. D. *J. Phys. Chem. B* **2006**, *110*, 2782.
(48) Berendsen, H. J. C.; Grigera, J. R.; Straatsma, T. P. *J. Phys. Chem.* **1987**, *91*, 6269.
(49) Martin, M. G.; Thompson, A. P. *Fluid Phase Equilib.* **2004**, *217*, 105.
(50) Chandler D. *Introduction to Modern Statistical Mechanics*; Oxford: New York, 1997; Chapter 6.

second water molecule ("water 2"), creating a water-separated SiO^-/H_3O^+ pair, at which point the deprotonation reaction is almost complete. This analysis appears consistent with insights from a transition path sampling AIMD simulation[11] as follows. The Figure 3d configuration, with the excess proton and the SiO^- separated by two hydrogen bonds, forms a possible free energy dividing surface between the intact and the deprotonated acid species, provided that the electric polarization between the two states, arising from the surrounding water molecules,[11] has sufficient time to equilibrate. Our simulation conditions allow such equilibration, and the excess proton is indeed observed to diffuse away if R fluctuates to regions significantly more negative than ca. −1.4 Å. Umbrella potentials of the type $(A/2)(R - R_o)^2$ are used to sample the reaction coordinate R. Just as significantly, they ensure that $R > -1.4$ Å and control the extent of proton transfer from "water 1" to all possible "water 2" so that at most a water-separated ion pair is obtained. Otherwise, if the excess proton is several hydrogen bonds removed from the SiO^- (say if it spends a significant amount of time on "water 3" via proton transfer from "water 2"), it can start to diffuse ("wander") through the simulation cell via the Grotthuss mechanism at O(1) ps time scale per proton transfer. With tens of H_2O molecules in the simulation cell and 10−20 ps trajectories, once the excess H^+ leaves the second hydration shell of the SiO^- it does not return and equilibrium sampling is not achieved. This "wandering" likely arises because the higher temperature and longer umbrella sampling trajectories than are generally used in the AIMD literature facilitate diffusion of the excess proton away from the SiO^-. Other deprotonation reaction coordinates used in the literature are discussed in the Supporting Information (section S2). They are found to give rise to wandering excess protons under our simulation conditions. As long as equilibrium sampling is achieved, the deprotonation free energy cost should not depend on the choice of coordinate.

To apply eq 1, we use a method similar to ref 8: finding the most probable optimal $O_{(water1)}-H^+$ hydrogen-bond distance r_{O-H} at each R, thus locally converting $W(R)$ to $\bar{W}(r_{O-H})$; performing a spline fit to the resulting $\bar{W}(r_{O-H})$; and integrating over r_{O-H} with a $4\pi r_{O-H}^2$ volume element, which takes place of the phase space factor $A(R)$ in eq 1. Equation 1 assumes that the entropic factors such as rotations of the reactant and products about the O−H axis are adequately sampled in the AIMD trajectories; otherwise, additional constraints and entropic factors are introduced.[51,52] Supporting Information section S2 shows that such constraints do not affect water autoionization free energies, partly because the variation in r_{O-H} needed to complete the deprotonation reaction is relatively small. Furthermore, we always reference predicted silanol pK_a to that of water autoionization[9] computed using the same reaction coordinate and elevated temperature. This minimizes systematic error arising from the simulation protocol (Supporting Information section S2), and phase space contributions approximately cancel out.

The metadynamics technique,[53−55] a promising and powerful alternative to umbrella sampling, has been applied to calculate dissociation free energies on surfaces[37] and acid−base reactions of small molecules.[10] This method, not yet implemented in VASP, can potentially be used for efficient comparative study of pK_a on other material surfaces after it has been adapted to deal with the wandering proton problem.

Gas-phase, high-level ab initio calculations are performed to check and correct chemical bonding energies predicted with the PBE functional used in the AIMD simulations. The Gaussian03 program suite is applied.[56] The pertinent sample chemical reaction is

$$Si(OH)_4 + H_2O\cdots OH^- \rightarrow Si(OH)_3O^-\cdots H_2O + H_2O \quad (2)$$

Geometries are optimized and harmonic vibrational frequencies computed with density functional theory using the B3LYP method[57,58] and the 6-311++G(d, p) basis set. At the B3LYP geometries, energies are computed with the coupled-cluster singles and doubles method including a perturbative correction for triple substitutions, CCSD(T),[59] using the aug-cc-pVDZ basis set. Basis set incompleteness corrections are added to the CCSD(T) energies. Finally, zero-point vibrational energy corrections computed from the B3LYP/6-311++G(d, p) frequencies are added. Using this protocol, the high-level ab initio calculation yields a reaction energy of −30.51 for eq 2. Gas-phase VASP-based PBE calculations, conducted with an energy cutoff identical to that in AIMD simulations, predict −27.17 kcal/mol. These numbers do not include the 2.24 kcal/mol zero-point energy (ZPE) corrections. Thus, the overall AIMD reaction energies should be corrected by a modest −1.10 kcal/mol. The basis set extrapolation procedure may have a systematic error larger than 1 pH unit (Supporting Information, section S3), but this does not affect the relative pK_a of different SiOH groups.

See the Supporting Information for details about constraints introduced to prevent proton attacks on SiO^-, the AIMD initialization protocol, further justifications for adopting the four-atom reaction coordinate, and extrapolating quantum chemistry results to the infinite basis set limit.

III. Results

Hydroxylated β-Cristobalite (100): Chemically Homogeneous SiOH. We first show that our simulation protocol predicts reproducible pK_a for chemically equivalent SiOH groups on the hydroxylated β-cristobalite (100) surface (Figure 2a). This well-studied model crystalline surface exhibits $\sigma_{SiOH} = 8$ nm^{-2}, larger than the experimental value of 4.6 nm^{-2} for amorphous silica.[2] At zero temperature, it features two types of Q^2 silanol groups: alternating hydrogen-bond donors and acceptors arranged in chains[60] (Figure 2a) not found in small molecules.[8−10] This feature is dynamically preserved in our finite-temperature, aqueous-phase simulations (Supporting Information, section S4).

Figure 4a shows that two chemically equivalent, hydrogen-bond-accepting SiOH groups on this surface are predicted to exhibit deprotonation $W(R)$ within 0.5 kcal/mol of each other. At large negative values of the reaction coordinate R, the deprotonated SiO^- is stabilized with three hydrogen bonds (i.e., $N_w = 3$, Figure 4b and 4c). At $R >$ ca. −0.8 Å, the SiO−H bond is only partially broken, $N_w < 3$, and the local $W(R)$ is not sensitive to the slight difference in N_w in the two simulations that arises from statistical noise. These observations appear consistent with a recent two-dimensional potential of mean force analysis of formic acid deprotonation.[10] Accounting for zero-point energy, correcting the AIMD functional with more accurate quantum chemistry methods, and referencing eq 1 to the water autodissociation constant $pK_w = 14$,[9] we estimate pK_a values of 7.5 and 7.7, close to the less acidic pK_a value reported

(51) Blumberger, J.; Klein, M. L. *Chem. Phys. Lett.* **2006**, *422*, 210.
(52) Leung, K.; Nielsen, I. M. B.; Criscenti, L. J. *J. Phys. Chem. B* **2007**, *111*, 4453.
(53) Laio, A.; Parrinello, M. *Proc. Natl. Acad. Sci. U.S.A.* **2002**, *99*, 12562.
(54) Iannuzzi, M.; Laio, A.; Parrinello, M. *Phys. Rev. Lett.* **2003**, *90*, 238302.
(55) Laio, A.; Gervasio, F. L. *Rep. Prog. Phys.* **2008**, *71*, 126601.
(56) Frisch, M. J. et al. *Gaussian 03*, Revision C.02; Gaussian Inc.: Wallingford, CT, 2004.
(57) Lee, C. T.; Yang, W. T.; Parr, R. G. *Phys. Rev. B* **1988**, *37*, 785.
(58) Becke, A. D. *J. Chem. Phys.* **1993**, *98*, 5648.
(59) Raghavachari, K.; Trucks, G. W.; Pople, J. A.; Head-Gordon, M. *Chem. Phys. Lett.* **1989**, *157*, 479.
(60) Yang, J.; Meng, S.; Xu, L. F.; Wang, E. G. *Phys. Rev. Lett.* **2004**, *92*, 146102.

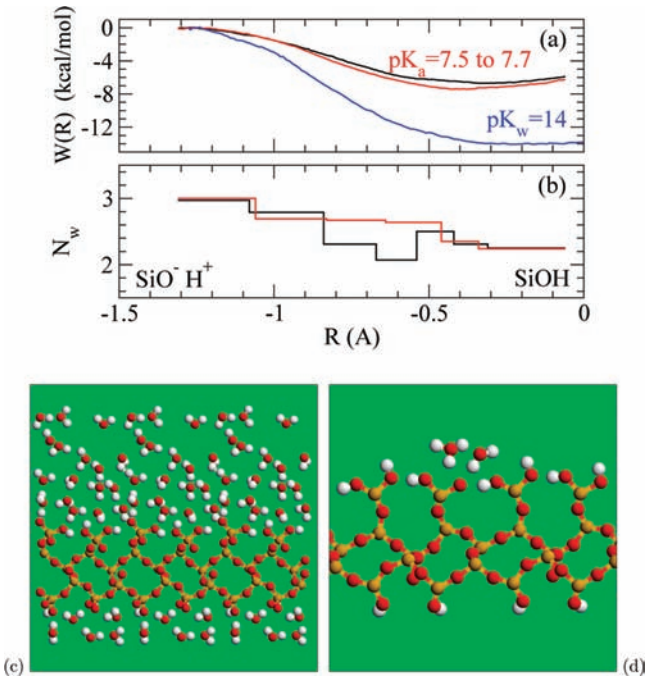

Figure 4. Deprotonation free energy on hydroxylated β-cristobalite (100) (Figure 2a). (a) Potential of mean force $W(R)$. The most negative R values represent SiO^-, while $R >$ ca. -0.8 Å indicates intact SiO−H bonds. Red and black lines: two different but chemically equivalent SiOH groups. Blue: water autoionization. (b) Mean hydration number, N_w, in each umbrella sampling window, defined as the number of protons within 2.5 Å (a typical hydrogen-bond distance) of the SiO^- oxygen. (c) Snapshot of the interface between water and hydroxylated β-cristobalite (100), replicated three times in the lateral direction. (d) Side view of the slab model with silanol groups forming hydrogen-bond chains, highlighting a Q^2, H-bonded SiO^- group in its representative hydrogen-bonding environment. Yellow, red, and white spheres depict Si, O, and H atoms, respectively.

by Ong et al.[16] The standard deviation is 0.3 pH unit. Multiple deprotonation on this surface is discussed in the Supporting Information, section S5.

Heterogeneity: Isolated, H-Bonded, Q^2, and Q^3 SiOH All Exhibit pK_a > 7. We next show that, contrary to previous hypotheses,[16,23−29] isolated, H-bonded, Q^2, and Q^3 silanol groups all exhibit pK_a > 7.0. We first create an isolated silanol group by replacing a hydrogen-bond-donating SiOH group on the hydroxylated β-cristobalite (100) surface with a SiH so that its neighboring SiOH group is no longer H-bonded (Figure 2b). Figure 5 shows that this isolated SiOH exhibits pK_a = 8.9 ± 0.3 and is less acidic by 1.2−1.4 pH units than when the SiOH hydrogen donor is present (Figure 2a). This is entropically reasonable because a hydrogen-bond-donating SiOH partner stabilizes the neighboring SiO^- alongside two water molecules, while three water molecules are required for an isolated SiO^-. AIMD correctly accounts for this effect because it models H_2O and SiOH on the same dynamical footing and because water−water and water−silanol hydrogen-bond energies are similar.[60] Hydroxyls on oxides with more ionic character than SiO_2 form stronger hydrogen bonds, and indeed, the relative abundance of interhydroxyl hydrogen bonding may partially be responsible for the crystal facet-dependent acidity of α-Al_2O_3.[61] This will be the subject of future comparative studies.

To compare Q^2 and Q^3 silanol groups, we reconstruct the hydroxylated β-cristobalite (100) surface by condensing every other pair of H-bonded SiOH groups into a SiOH and a H_2O molecule (Figure 2c). This involves the elimination of a hydrogen-bond-donating OH group plus the proton on its adjacent, hydrogen-bond-accepting SiOH (Figure 2d). The resulting undercoordinated Si and O atoms are joined together to form a covalent bond, in the process pulling apart the remaining H-bonded SiOH pairs so they are now isolated from one another. A similar structural motif has been considered in the literature.[62] This surface has $\sigma_{SiOH} = 4$ nm^{-2}, with all SiOH groups being Q^3, isolated, and residing on silica rings containing at least 5 Si atoms. Such rings should be unstrained, unlike 3-membered $(Si-O)_3$ rings discussed below. The pK_a is found to be 8.1 ± 0.5 (Figure 5).

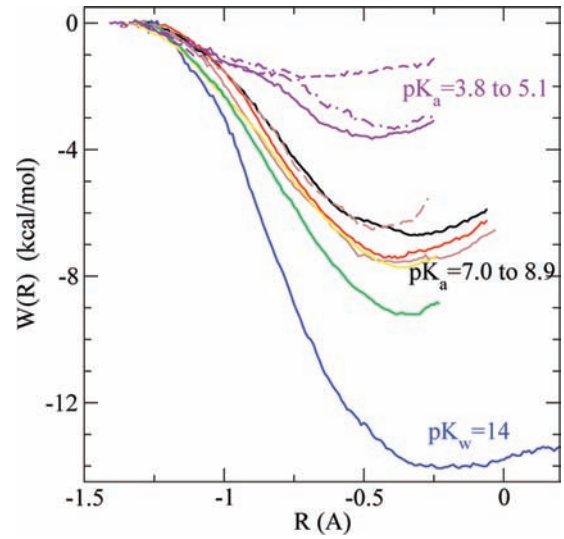

Figure 5. Distribution of pK_a. Black and red lines: $W(R)$ for SiOH on the hydroxylated β-cristobalite (100) surface (Figure 2a). Green: same surface but with hydrogen-bond-donating SiOH artificially removed (Figure 2b). Brown, solid and dashed: reconstructed β-cristobalite (100) (Figure 2c) with 6 and 4 layers of water in the simulation cell, respectively. Yellow: $(H_3SiO)_3SiOH$ (Figure 2e). Violet: reconstructed quartz (0001) (Figure 2f) with the SiOH residing on a silica trimer ring (solid) or otherwise (dashed and dot-dashed). Blue: $W(R)$ for water autoionization.

We also consider a $(SiH_3)_3SiOH$ molecule featuring an isolated, Q^3 SiOH group (Figure 2e), which exhibits a comparable pK_a = 7.9 ± 0.5. Thus, in general, Q^3 and Q^2 silanol groups do not exhibit pK_a's that differ by 4 pH units as previously proposed.[23−29] Over the range 4 nm^{-2} ≤ σ_{SiOH} ≤ 8 nm^{-2}, the precise value of σ_{SiOH} has little effect on pK_a.

To some extent, all our crystalline silica models are nanoslits with thin water slabs confined between the surfaces. As the water content decreases, the dielectric solvation of SiO^- and H^+ species should decrease while intact SiOH groups should be weakly affected. Thus, one expects a lower acidity and a higher pK_a in strongly nanoconfined aqueous media.[63] To examine confinement effects, a pK_a calculation is performed for a smaller reconstructed β-cristobalite (100) simulation cell, 20 Å in the z direction, containing 4 layers of water. This system actually yields a lower pK_a = 7.0 ± 0.4 but is lower only by 1.1 pH units (dashed brown line in Figure 5). It is possible the unexpected pK_a decrease between the 6- and 4-water layer models arises from anomalies in the hydrogen-bonding network

(61) Fitts, J. P.; Shang, X. M.; Flynn, G. W.; Heinz, T. F.; Eisenthal, K. B. *J. Phys. Chem. B* **2005**, *109*, 7981.

(62) Chuang, I.-S.; Maciel, G. E. *J. Phys. Chem. B* **1997**, *101*, 3052.

(63) Preliminary experimental measurements suggest that the pH of zero charge increases inside narrow silica nanoporour membranes (Jiang, Y.-B. Private communications).

not apparent from visual inspection of water configurations. The water density is also affected by the confinement.[64] In the 4-layer model, all water molecules are at most two layers away from the crystalline silica surfaces, and AIMD conducted with GCMC-predicted water content is found to yield a second layer H_2O density that is 18% above 1.0 g/cm^3. However, this is unlikely to change the dielectric response sufficiently to lower the pK_a by 1 unit. Assuming one can apply the Born hydration formula for excess proton hydration in this heterogeneous medium, $\Delta G_{hyd} \sim X(1 - 1/\varepsilon_o)$, where $X \sim -264$ kcal/mol for the proton.[65] If the 6 layers of water have $\varepsilon_o = 80$, the 4-layer system must exhibit $\varepsilon_o = 140$ to make hydration more favorable by 1 pH unit when in fact confinement generally reduces the dielectric constant of water.[12] In any case, the discrepancy in pK_a is actually within two standard deviations and may simply arise from statistical uncertainties. This test suggests that confinement effects are not large for the slit pore geometry[3] down to about 1 nm slit widths. Therefore, our reported pK_a for 6-water layer systems should be good approximations of pristine crystalline silica surfaces in contact with bulk liquid water. We also stress that all slab geometries in Figure 2a−c have been studied using 6-water layer simulation cells, and their *relative* pK_a should be mostly free of system size effects. However, two-dimensional confinement in cylindrical amorphous silica nanopores[12,23,66−68] may have a stronger impact on pK_a.[63]

High Acidity and Chemical Reactions on Strained Reconstructed Quartz Surfaces. Finally, it seems imperative to demonstrate the possibility of an unusually acidic silanol group. The following "computational existence proof" is necessarily more speculative than the conclusions about Q^2, Q^3, isolated, and H-bonded SiOH pK_a discussed above, but it emphasizes the likely role of defected regions when accounting for pK_a = 4.5.

Having considered $\sigma_{SiOH} = 8$ and 4 nm^{-2}, we examine an even lower SiOH surface density. A recent experimental study has attached crystal violet dyes to deprotonated silanol groups. On the basis of the flat, 120 nm^2 surface area of the dye molecule, it is proposed that strong acidity is correlated with local SiOH surface density $\sigma_{SiOH} < 0.83$ nm^{-2}.[22] In our DFT calculations, the optimal geometry of crystal violet when covalently bonded to $(HO)_3SiO^-$ is not flat but is substantially distorted. However, this suggestion of low SiOH surface density being associated with the more acidic SiOH appears consistent with other experimental and theoretical observations discussed below.

Since most cuts through crystalline forms of silica yield surfaces with substantial hydroxylation,[69] we investigate a reconstructed, completely dehydroxylated quartz (0001) model, featuring $(Si-O)_3$ trimer rings, predicted to be metastable in vacuum.[70,71] The 2.3 SiOH groups per square nanometer are reintroduced by removing two surface Si atoms and performing further reconstruction and hydroxylation to keep all atoms fully coordinated. This yields two types of silanol groups which are hydrogen bonded to each other; one member of the pair resides on a cyclic trimer, while the other does not (Figure 2f). Regions devoid of SiOH and dominated by siloxane (Si−O−Si) bridges are hydrophobic, and this model surface may therefore be consistent with hydroxyl groups in hydrophobic pores reported to be unusually acidic on other oxides.[72] We conduct one deprotonation umbrella sampling simulation of a silanol group residing on a cyclic trimer (Figure 5, solid violet curve) and two simulations where the SiOH does not reside on a trimer (dashed and dot−dashed violet). Figure 5 indeed shows that these SiOH groups exhibit p$K_a \sim 5.1 \pm 0.3$, 4.8 ± 0.4, and 3.8 ± 0.4, respectively, close to the experimental value of 4.5. More significantly, their average pK_a values are separated from the median of all other SiOH groups previously examined in this work by 3.4 pH units.

Unlike cyclic silica tetramers or larger Si−O rings, cyclic silica trimers are strained.[1,74,75] At zero temperature, in the absence of water, the Si atom of the SiOH group residing on a silica trimer ring exhibits Si−O−Si angles of 137.5°, 130.4°, and 132.0°. For the SiOH group not residing on a silica trimer, the angles are 154.9°, 131.8°, and 147.8°. A few of these angles deviate substantially from the ideal, unstrained Si−O−Si value of approximately 145°. This likely accounts for the low pK_a computed for these SiOH groups. Other trimer rings not decorated with SiOH are also strained, and the slow spatial decay of their surface strain fields[73] may also contribute to the high acidity of SiOH group not residing on them.

Within hours in moist air,[1,74,75] cyclic trimer-containing surfaces are known to incorporate water and break open to reduce strain and increase the local σ_{SiOH}. At the water-reconstructed quartz interface, during umbrella sampling deprotonation of the SiOH group residing on a 3-membered ring (Figure 2f), we indeed observe a water molecule forming a transient bond with another Si atom on a Si−O trimer 6 Å away from the tagged SiO^- within picoseconds (Figure 6b). The resulting 5-coordinated Si has been observed in simulations[71,76,77] and found to be the intermediate in the trimer ring-opening mechanism on wet silica amorphous surfaces in reactive force field and molecular orbital calculations.[76−78] Our AIMD trajectories show that this mechanism remains operative at explicit liquid water−silica interfaces; proton hopping via the Grotthuss mechanism occurs readily, enabling the H_2O adsorbed on the surface Si to lose a proton to bulk water, forming a new SiOH group within ~10 ps (Figure 6c). Then, in 2 of the 4 sampling windows, a Si−O bond on the now 5-coordinated Si breaks to open the OH-incorporated $(Si-O)_3$ ring and irreversibly introduce another new SiOH (Figure 6d). Our trajectories thus differ from a recent molecular dynamics study of the liquid water-reconstructed quartz interface, where the adsorbed water molecule, not described by a reactive force field, ultimately

(64) Xu, S.; Scherer, G. W.; Mahadevan, T. S.; Garofalini, S. H. *Langmuir* **2009**, *25*, 5076, and references therein.
(65) Tissandier, M. D.; Cowen, K. A.; Feng, W. Y.; Grunlach, E.; Cohen, M. H.; Earhart, A. D.; Coe, J. V.; Tuttle, T. R. *J. Phys. Chem. A* **1998**, *102*, 7787.
(66) Hartnig, C.; Witschel, W.; Spohr, E.; Gallo, P.; Ricci, M. A.; Rovere, M. *J. Mol. Liq.* **2000**, *85*, 127.
(67) Cruz-Chu, E. R.; Aksimentiev, A.; Schulten, K. *J. Phys. Chem. B* **2006**, *110*, 21497.
(68) Leung, K. *J. Am. Chem. Soc.* **2008**, *130*, 1808.
(69) Nangia, S.; Washton, N. M.; Mueller, K. T.; Kubicki, J. D.; Garrison, B. J. *J. Phys. Chem. C* **2007**, *111*, 5169.
(70) Du, Z. M.; de Leeuw, N. H. *Surf. Sci.* **2004**, *554*, 193.
(71) Du, Z. M.; de Leeuw, N. H. *Dalton Trans.* **2006**, *22*, 2623.
(72) Braunschweig, B.; Eissner, S.; Daum, W. *J. Phys. Chem. C* **2008**, *112*, 1751.
(73) Rickman, J. M.; Srolovitz, D. J. *Surf. Sci.* **1993**, *284*, 211.
(74) Brinker, C. J.; Kirkpatrick, R. J.; Tallant, D. R.; Bunker, B. C.; Montez, B. *J. Non-Cryst. Solids* **1988**, *99*, 418.
(75) Wallace, S.; West, J. K.; Hench, L. L. *J. Non-Cryst. Solids* **1993**, *152*, 101.
(76) Garofalini, S. H. *J. Non-Cryst. Solids* **1990**, *120*, 1.
(77) Mahadevan, T. S.; Garofalini, S. H. *J. Phys. Chem. C* **2008**, *112*, 1507.
(78) Lasaga, A. C. *Rev. Mineral.* **1990**, *23*, 17.

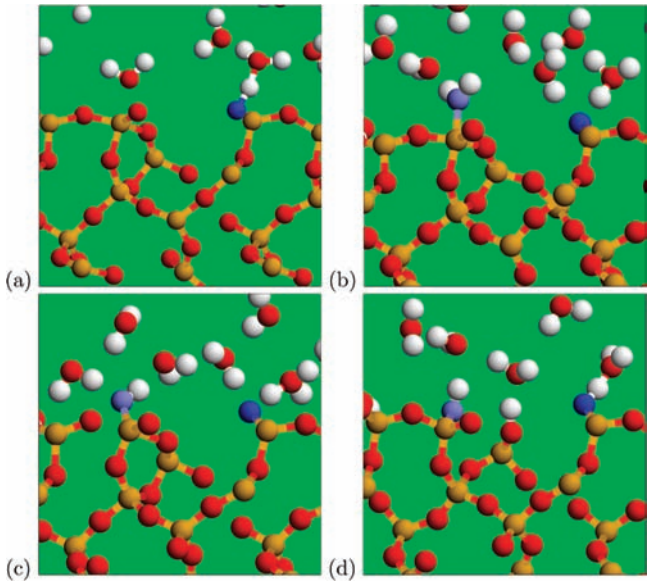

Figure 6. Water incorporation onto reconstructed quartz. (a) Initial equilibrated snapshot of the SiO^-H^+ contact ion pair on the reconstructed quartz (0001) surface where the SiO^- resides on a 3-membered ring (truncated in this figure). The tagged SiO^- oxygen is in deep blue; its H-bond SiOH donor is out of the frame. All other Si, O, and H atoms are in yellow, red, and white, respectively. (b) Snapshot after ~3 ps. To the left of the SiO^-, a water molecule (light blue) has attached itself to a Si atom on another silica trimer ring, which is unhydroxylated. That Si becomes 5-coordinated. (c) This water molecule loses a proton to bulk water; one of the Si−O bonds not on the trimer ring becomes stretched. This is reversible as long as another SiOH is not created. (d) In another sampling window for this SiOH, the trimer ring breaks open instead, forming a new SiOH after extracting a proton from water.

desorbs from the 5-coordinated surface Si atom without inducing chemical reactions.[71]

These irreversible side reactions prevent strict equilibrium sampling needed for $W(R)$ calculations. Fortunately, for the SiOH residing on a cyclic trimer (Figure 6), analysis of the pre- and post-ring-breaking statistics reveals that the nearby chemical reaction has little effect on its pK_a. We further analyze trimer ring-opening effects on the pK_a of another SiOH group, this one not residing on a surface 3-membered ring. A H_2O incorporation reaction also occurs in the neighborhood of this tagged SiOH (Figure 7). We split the sampling windows into two groups: (A) those without irreversible hydrolysis of a nearby silica ring (Figure 7a) and (B) those with trimer ring breaking and formation of two new SiOH groups (Figure 7b). Then two complete sets of sampling windows spanning the entire deprotonation pathway are spawned from these seed windows, yielding two pK_a: case A, pK_a = 3.8 (Figure 5, dashed violet curve), and case B, pK_a = 4.8 (Figure 5, dot−dashed violet). The results show that H_2O incorporation and a single ring-breaking event nearby does appear to increase the pK_a of the tagged SiOH not residing on a trimer ring. However, the increase is only 1.0 pH unit, almost within statistical uncertainties. In case A, the three Si−O−Si angles on the silica trimer ring average to 121.1°, 134.0°, and 132.2° along the trajectory; the first refers to the angle where both Si are below the silica surface ("buried"). In case B, this angle linking the buried Si atoms relaxes significantly to 140.5°. The second angle, which involves the surface Si and a buried Si, remains almost unchanged at 136.0°. (The third linkage is destroyed during ring opening.) Si atoms which no longer participate in strained Si−O−Si linkages should be more stable against H_2O attack.

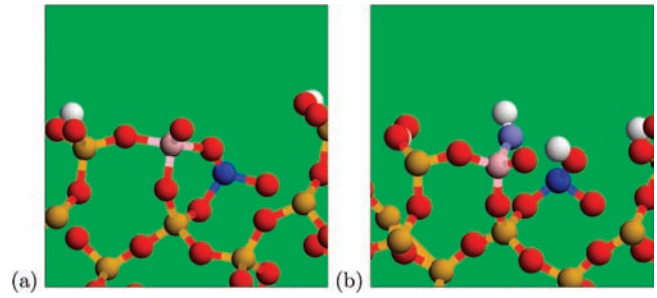

Figure 7. Trimer silica ring and Si−O−Si angles. Configurations are taken from AIMD pK_a calculations where the SiOH group involved in the pK_a calculation does not reside on a silica trimer ring. That tagged SiOH is off frame; all H_2O molecules are removed for clarity. (a) Snapshot along the AIMD trajectory where the 3-membered ring remains intact (case A). The 3 Si−O−Si angles within the ring average to 121.1° (between Si atoms on the trimer ring colored yellow and dark blue), 134.0° (yellow/pink), and 132.2° (pink/dark blue). (b) Incorporation of a H_2O (its oxygen colored light blue) opens the ring (case B). The surviving Si−O−Si angles are 140.5° (yellow/dark blue) and 136.0° (yellow/pink). O and H atoms are represented by red and white spheres, respectively.

From these considerations, we conclude that despite interference from H_2O incorporation reactions there remains a statistically significant difference in the pK_a's on this surface and the pK_a's ranging from 7.0 to 8.9 for all other silanol groups investigated before (Figure 5). This finding suggests that strain, low local silanol surface density, hydrophobicity, and low pK_a are correlated on amorphous silica surfaces. Indeed, atomistic model surfaces with low local σ_{SiOH} regions almost always exhibit 3-membered rings.[70,76,79] These regions may be in dynamic equilibrium with solvated silica fragments in solution, constantly being dissolved/hydrolyzed and reconstituted when dissolved fragments renucleate on hydroxylated regions.[71,80−82] The dynamic equilibrium has recently been demonstrated in Monte Carlo simulations[81] using a reactive silica force field.[83]

We only have observed one ring-opening reaction on each surface. The limited AIMD trajectory length does not conclusively allow us to predict how many trimer rings persist at the liquid water−amorphous silica interface as a function of time. Therefore, we do not definitively assign this structure to the observed pK_a = 4.5 SiOH group and instead pose it as a challenge to experimental work, including single-molecule spectroscopy,[84] to determine whether they are sufficiently abundant over time to account for the 19% of all silanol groups shown to exhibit high acidity.[16,17] We also point out that while cyclic silica trimers are well known to react with moist air, other popular crystalline silica model surfaces should also be hydrolytically unstable.[20] Thus, the hydroxylated α-quartz (0001) and β-cristobalite (100) surfaces, with $\sigma_{SiOH} \sim 9$ and 8 nm^{-2}, respectively, are often used as models to study the interface between liquid water and generic silica solids in classical MD simulations. However, if these simulations permit chemical reactions over long enough times, we speculate that some of the SiOH groups on such surfaces may also react with water[20,81]

(79) Hassanali, A. A.; Singer, S. J. *J. Phys. Chem. B* **2007**, *111*, 11181. see Fig. 9.
(80) Criscenti, L. J.; Kubicki, J. D.; Brantley, S. L. *J. Phys. Chem. A* **2006**, *110*, 198.
(81) Nangia, S.; Garrison, B. J. *J. Am. Chem. Soc.* **2009**, *131*, 9538.
(82) Trinh, T. T.; Jansen, A. P. J.; van Santen, R. A.; Meijer, E. J. *J. Phys. Chem. C* **2009**, *113*, 2647.
(83) Feuston, B. P.; Garofalini, S. H. *J. Chem. Phys.* **1988**, *89*, 5818.
(84) Fu, Y.; Collinson, M. M.; Higgins, D. A. *J. Am. Chem. Soc.* **2004**, *126*, 13838.

in a way to reduce the silanol surface density toward the amorphous silica $\sigma_{SiOH} = 4.6\ nm^{-2}$ observed in experiments.[2,30]

IV. Discussion

AIMD-based potential of mean force calculations simulations have been demonstrated to yield reproducible pK_a for chemically equivalent silanol groups. The statistical uncertainties of our simulation protocol are estimated to be about 0.3−0.5 pH units, consistent with explicit calculations on two chemically equivalent SiOH. Therefore these simulations should reliably distinguish the relative pK_a of heterogeneous SiOH groups 4 pH units apart. Resolving hydroxyl pK_a on other surfaces may remain a challenge if the acidities are less widely separated.

Our pK_a calculations suggest that comparative studies between SiO_2 and other material surfaces will be extremely interesting. One intriguing candidate surface is a quartz surface densely functionalized with carboxylic acid groups. To our knowledge, this is the only other material surface which clearly exhibits bimodal pK_a behavior.[85] Other candidates are the different facets of crystalline alumina, which may feature several pK_a's unresolved into distinct, measurable components.[72,86,87] Structural motifs such as chemical connectivity and interhydroxyl hydrogen bonding have also been invoked to explain the pK_a in these systems; as mentioned in the text, interhydroxyl hydrogen bonding may affect the pK_a of the more ionic Al_2O_3 surfaces more strongly than on any form of silica surfaces. See the Supporting Information, section S6, for more details on these material systems. Finally, SFVG spectra[17] and time-dependent acid−base phenomena on quartz[88] can also be investigated in the future.

V. Conclusions

In this paper, we have performed AIMD pK_a calculations on five representative crystalline silica surfaces plus a molecular system exhibiting different silanol (SiOH) structural motifs. From the results, we have conclusively shown that the more acidic of the two pK_a observed in experiments cannot, as previously proposed,[22−29] be explained by the existence of silanol groups with certain chemical connectivities or intersilanol hydrogen bonding. In fact, we find p$K_a \sim 4.5$ silanol groups only on strained surfaces with sparse silanol coverage. While our demonstration of the existience of such low pK_a SiOH groups is necessarily somewhat speculative, this study highlights the role of defected regions as the most promising candidate to explain the elusive bimodal acid−base behavior of silica surfaces.[16−18] Assigning structural motifs to the more strongly acidic SiOH groups is particularly crucial in nonreactive force-field-based modeling of silica nanofluidic channels, where the preferentially deprotonated SiOH sites at neutral pH have to be assigned in a static way.[12,23,66,67,89,90] In the process of studying the acid−base behavior, we also observe irreversible, water-assisted ring-opening reactions of strained silica trimer rings in contact with liquid water. The reaction was previously studied on wet silica surfaces;[76,76,78] our AIMD simulations demonstrate that a similar mechanism is operative at liquid water−silica interfaces.

Acknowledgment. We thank Ron Shen, Stephen Garofalini, Susan Rempe, Jeff Brinker, Dave Tallant, Ying-Bing Jiang, and Franz Geiger for discussions. This work was supported by the Department of Energy under Contract DE-AC04-94AL85000. Sandia is a multiprogram laboratory operated by Sandia Corporation, a Lockheed Martin Company, for the U.S. Deparment of Energy. L.J.C. acknowledges support from the U.S. DOE Office of Basic Energy Sciences, Division of Chemical Sciences, Geosciences, and Biosciences.

Supporting Information Available: Further information is provided regarding details of the AIMD simulations, justification for the reaction coordinate used, quantum chemistry calculations (including all energies and optimized geometries), the dynamics of hydrogen-bond fluctuations on silica surfaces, proton exchange due to multiple deprotonation, and a brief overview of acid−base behavior in alumina- and carboxylate-acid-functionalized surfaces. This material is available free of charge via the Internet at http://pubs.acs.org.

JA906190T

(85) Konek, C. T.; Musorrafiti, M. J.; Al-Abadleh, H. A.; Bertin, P. A.; Nguyen, S. T.; Geiger, F. M. *J. Am. Chem. Soc.* **2004**, *126*, 11754.
(86) Zhang, L.; Tian, C.; Waychunas, G. A.; Shen, Y. R. *J. Am. Chem. Soc.* **2008**, *130*, 7686.
(87) Stack, A. G.; Higgins, S. R.; Eggleston, C. M. *Geochim. Cosmochim. Acta* **2001**, *65*, 3055.
(88) Gibbs-Davis, J. M.; Kruk, J. J.; Konek, C. T.; Scheidt, K. A.; Geiger, F. M. *J. Am. Chem. Soc.* **2008**, *130*, 15444.
(89) Cruz-Chu, E. R.; Aksimentiev, A.; Schulten, K. *J. Phys. Chem. C* **2009**, *113*, 1850.
(90) Leung, K.; Rempe, S. B. *J. Comput. Theor. Nanoscience* **2009**, *6*, 1948.